INSTITUTE OF PHYSICS PUBLISHING INVERSE PROBLEMS

Inverse Problems **17** (2001) 1997–2015 PII: S0266-5611(01)24318-4

The direct and inverse scattering problems for partially coated obstacles

Fioralba Cakoni, David Colton and Peter Monk

Department of Mathematical Sciences, University of Delaware, Newark, DE 19716, USA

E-mail: monk@math.udel.edu

Received 27 April 2001, in final form 4 October 2001
Published 15 November 2001
Online at stacks.iop.org/IP/17/1997

Abstract

We consider the direct and inverse scattering problems for partially coated obstacles. To this end, we first use the method of integral equations of the first kind together with variational methods to solve a scattering problem for the Helmholtz equation where the scattered field satisfies mixed Dirichlet-impedance boundary conditions on the Lipschitz boundary of the scatterer D. We then use the linear sampling method to solve the inverse scattering problem of determining D from a knowledge of the far-field pattern of the scattered field. Numerical examples are given showing the performance of the linear sampling method in this case.

1. Introduction

The inverse scattering problem for acoustic or electromagnetic waves has drawn increased attention in recent years due its importance in various areas of imaging and non-destructive testing [1]. Until recently the main techniques for solving such problems have been some form of a 'weak scattering' approximation or an appropriately designed nonlinear optimization algorithm. Unfortunately, for their practical implementation, both of these approaches depend on knowing the boundary condition satisfied by the field on the surface of the scatterer and in those areas of application involving 'hostile' targets this is, in general, unknown. In particular, such targets are typically coated by some material on a portion of the boundary and, since both the material and extent of the coating are unknown, the boundary condition is also unknown. More recently, a method for solving the inverse scattering problem has been developed which does not depend on a knowledge of the boundary condition satisfied by the field on the boundary of the scatterer [2–4, 9]. This new method, called the *linear sampling method*, is well suited to the problem of detecting partially coated hostile targets and it is the purpose of this paper to show how this can be done.

To fix our ideas, we consider the scattering of an electromagnetic time harmonic plane wave by a perfectly conducting infinite cylinder with Lipschitz boundary, that is partially

0266-5611/01/061997+19$30.00

coated by material with surface impedance λ. Assuming that the electric field is polarized in the TM mode this leads to a mixed boundary value problem for the Helmholtz equation in $\mathbb{R}^2$. This direct scattering problem will be considered in section 2 of this paper using the method of integral equations of the *first* kind as discussed in [11]. Here we prove two results that are required in our analysis of the inverse problem. We will then examine in section 3 the inverse scattering problems of determining the cross section D of the infinite cylinder from a knowledge of the far-field pattern of the scattered wave. This examination is based on showing the validity of the linear sampling method for mixed boundary value problems in scattering theory. Included in our discussion is an analysis of the linear sampling method for sampling points z that are either in D or $\mathbb{R}^2 \setminus \overline{D}$ (previous discussions of the linear sampling method in [3] and [4] only considered the case when $z \in D$). Finally, in section 4, we will show how the linear sampling method for mixed boundary value problems can be numerically implemented and provide several numerical examples of reconstruction of scattering obstacles from a knowledge of (noisy) far-field data.

2. Direct scattering problem

Let $D \subset \mathbb{R}^2$ be a bounded region with Lipschitz boundary Γ such that $\mathbb{R}^2 \setminus \overline{D}$ is connected. We assume that the boundary Γ has a Lipshitz dissection $\Gamma = \Gamma_D \cup \Pi \cup \Gamma_I$, where Γ_D and Γ_I are disjoint, relatively open subsets of Γ, having Π as their common boundary in Γ (see e.g. [11]). Furthermore, boundary conditions of Dirichlet and impedance type are specified on Γ_D and Γ_I, respectively. Let ν denote the unit outward normal vector defined almost everywhere on $\Gamma_D \cup \Gamma_I$.

We consider the two-dimensional scattering problem of determining the total field $U(x) = u(x) + \mathrm{e}^{\mathrm{i}kx\cdot d}$, given as the sum of the unknown scattered wave and incident plane wave, from the exterior mixed boundary value problem

$$\Delta U + k^2 U = 0 \qquad \text{in} \quad \mathbb{R}^2 \setminus \overline{D} \tag{1a}$$

$$U = 0 \qquad \text{on} \quad \Gamma_D \tag{1b}$$

$$\frac{\partial U}{\partial \nu} + \mathrm{i}k\lambda U = 0 \qquad \text{on} \quad \Gamma_I, \tag{1c}$$

where $k > 0$ is the wavenumber, λ is a positive constant, $x \in \mathbb{R}^2$, and d is a unit vector describing the incident direction. Moreover, the scattered field u is required to satisfy Sommerfeld radiation condition [1]

$$\lim_{r\to\infty} \sqrt{r}\left(\frac{\partial u}{\partial r} - \mathrm{i}ku\right) = 0, \tag{2}$$

uniformly in $\hat{x} = x/|x|$ with $r = |x|$.

In order to formulate the scattering problem (1*a*)–(2) more precisely we need to recall the definition of the following Sobolev spaces. Let $\Gamma_0 \subseteq \Gamma$ be a piece of the boundary. If $H^1(D)$, $H^1_{\mathrm{loc}}(\mathbb{R}^2 \setminus \overline{D})$ denote the usual Sobolev spaces and $H^{1/2}(\Gamma)$ their usual trace space, then we define

$$H^{1/2}(\Gamma_0) := \{u|_{\Gamma_0} : u \in H^{1/2}(\Gamma)\}$$
$$\tilde{H}^{1/2}(\Gamma_0) := \{u \in H^{1/2}(\Gamma) : \ \operatorname{supp} u \subseteq \overline{\Gamma}_0\}$$
$$H^{-1/2}(\Gamma_0) := (\tilde{H}^{1/2}(\Gamma_0))' \text{ the dual space of } \tilde{H}^{1/2}(\Gamma_0)$$
$$\tilde{H}^{-1/2}(\Gamma_0) := (H^{1/2}(\Gamma_0))' \text{ the dual space of } H^{1/2}(\Gamma_0).$$

We can now define the following mixed boundary value problems:

Exterior mixed boundary value problem

Let $f \in H^{1/2}(\Gamma_D)$ and $h \in H^{-1/2}(\Gamma_I)$. Find a function $u \in H^1_{\mathrm{loc}}(\mathbb{R}^2 \setminus \overline{D})$ such that

$$\Delta u + k^2 u = 0 \qquad \text{in} \quad \mathbb{R}^2 \setminus \overline{D} \tag{3a}$$

$$u = f \qquad \text{on} \quad \Gamma_D \tag{3b}$$

$$\frac{\partial u}{\partial \nu} + \mathrm{i}\lambda k u = h \qquad \text{on} \quad \Gamma_I \tag{3c}$$

$$\lim_{r\to\infty} \sqrt{r}\left(\frac{\partial u}{\partial r} - \mathrm{i}ku\right) = 0. \tag{3d}$$

We will also need to consider the corresponding interior mixed boundary value problem.

Interior mixed boundary value problem

Let $f \in H^{1/2}(\Gamma_D)$ and $h \in H^{-1/2}(\Gamma_I)$. Find a function $u \in H^1(D)$ such that

$$\Delta u + k^2 u = 0 \qquad \text{in} \quad D \tag{4a}$$

$$u = f \qquad \text{on} \quad \Gamma_D \tag{4b}$$

$$\frac{\partial u}{\partial \nu} + \mathrm{i}k\lambda u = h \qquad \text{on} \quad \Gamma_I. \tag{4c}$$

The solution of the above mixed boundary value problems is well defined in the corresponding variational spaces, namely

$$\mathcal{L}_{\mathrm{ext}} := \{v \in H^1_{\mathrm{loc}}(\mathbb{R}^2 \setminus \overline{D}) : \Delta v + k^2 v = 0 \text{ in the distributional sense, satisfying } (3d)\}$$

for the exterior problem, and

$$\mathcal{L}_{\mathrm{int}} := \{v \in H^1(D) : \Delta v + k^2 v = 0 \text{ in the distributional sense}\}$$

for the interior problem.

Hence, the variational formulation for the exterior problem reads: find $u \in H^1_{\mathrm{loc}}(\mathbb{R}^2 \setminus \overline{D})$ with $u|_{\Gamma_D} = f$ such that for all test functions $v \in H^1(\mathbb{R}^2 \setminus \overline{D})$ with compact support in $\mathbb{R}^2$ and $v|_{\Gamma_D} = 0$ we have

$$-k^2 \int_{\mathbb{R}^2 \setminus \overline{D}} u\bar{v}\,\mathrm{d}x + \int_{\mathbb{R}^2 \setminus \overline{D}} \nabla u \cdot \nabla \bar{v}\,\mathrm{d}x = -\langle h, \bar{v}|_{\Gamma_I}\rangle + \mathrm{i}k\lambda(u, v)_{\Gamma_I}, \tag{5}$$

where $\langle \cdot, \cdot \rangle$ denotes the duality pair $H^{-1/2}(\Gamma_I)$, $\tilde{H}^{1/2}(\Gamma_I)$ and $(\cdot, \cdot)$ the usual $L^2(\Gamma_I)$ scalar product. In addition u is required to satisfy the radiation condition $(3d)$ which can be written

$$\lim_{R\to\infty} \int_{|x|=R} \left|\frac{\partial u}{\partial R} - \mathrm{i}ku\right|^2 \mathrm{d}s = 0.$$

Similarly, for the interior problem we want to find $u \in H^1(D)$ with $u|_{\Gamma_D} = f$ such that for all test functions $v \in H^1(D)$ and $v|_{\Gamma_D} = 0$ we have

$$-k^2 \int_D u\bar{v}\,\mathrm{d}x + \int_D \nabla u \cdot \nabla \bar{v}\,\mathrm{d}x = \langle h, \bar{v}|_{\Gamma_I}\rangle - \mathrm{i}k\lambda(u, v)_{\Gamma_I}.$$

Theorem 2.1. *The interior mixed boundary value problem (4a)–(4c) has at most one solution in* $\mathcal{L}_{\mathrm{int}}$.

Proof. Let u be a solution of (4*a*)–(4*c*) with $f \equiv 0$ and $h \equiv 0$. Then an application of Green formula in D yields

$$-k^2 \int_D |u|^2 \, \mathrm{d}x + \int_D |\nabla u|^2 \, \mathrm{d}x = \int_\Gamma \frac{\partial u}{\partial \nu} \bar{u} \, \mathrm{d}s, \tag{6}$$

and making use of homogeneous boundary condition we obtain

$$-k^2 \int_D |u|^2 \, \mathrm{d}x + \int_D |\nabla u|^2 \, \mathrm{d}x = -\mathrm{i}k\lambda \int_{\Gamma_I} |u|^2 \, \mathrm{d}s \, . \tag{7}$$

Since k and λ are real numbers, by taking the imaginary part of (7) we conclude that $u|_{\Gamma_I} \equiv 0$ as a function of $H^{1/2}(\Gamma_I)$ and consequently $\frac{\partial u}{\partial \nu}\big|_{\Gamma_I} \equiv 0$ as a function of $H^{-1/2}(\Gamma_I)$.

Now let B_ρ be a ball of radius ρ with centre on Γ_I such that $\overline{B}_\rho \cap \Gamma_D = 0$ and define $v = u$ in $D \cap B_\rho$, $v = 0$ in $(\mathbb{R}^2 \setminus \overline{D}) \cap B_\rho$. Then applying Green's second identity in each of these domains to v and a test function $\varphi \in C_0^\infty(B_\rho)$ we see that v is a weak solution of Helmholtz equation in B_ρ. Thus v is a classical solution in B_ρ (see [11]) and hence real-analytic in B_ρ. We can now conclude that $u \equiv 0$ in B_ρ and thus $u \equiv 0$ in D. □

Theorem 2.2. *The exterior mixed boundary value problem (3a)–(3d) has at most one solution in* $\mathcal{L}_{\text{ext}}$.

Proof. By doing the same as in the previous theorem but in the domain $(\mathbb{R}^2 \setminus \overline{D}) \cap B_R$, with B_R a ball of radius $R > 0$ containing D, the result follows through the use of Rellich's lemma [1]. □

The estimate in the following theorem will play a central role in the proof of theorem 3.1 in the following section.

Theorem 2.3. *The interior mixed boundary value problem (4a)–(4c) has a weak solution in* $\mathcal{L}_{\text{int}}$. *Moreover, the solution satisfies the estimate*

$$\|u\|_{H^1(D)} \leqslant C(\|f\|_{H^{1/2}(\Gamma_D)} + \|h\|_{H^{-1/2}(\Gamma_I)}) \tag{8}$$

with C a positive constant.

Proof. The proof is based on the method first used by Hsiao and Wendland [7, 8], and Nédélec [12] for the Laplace equation. However, for details and a systematic representation we refer to the book of McLean [11].

We first reformulate the interior mixed boundary problem (4*a*)–(4*c*) as a 2×2 system of boundary integral equation of the first kind. We start with the Green representation formula of a weak solution

$$u = \mathcal{S}\frac{\partial u}{\partial \nu} - \mathcal{D}u, \tag{9}$$

where the bounded operators

$$\mathcal{S} : H^{-1/2}(\Gamma) \longrightarrow H^1(D) \qquad \mathcal{D} : H^{1/2}(\Gamma) \longrightarrow H^1(D)$$

defined by

$$\mathcal{S}\phi(x) := \int_\Gamma \psi(y)\Phi(x, y) \, \mathrm{d}s_y, \qquad x \in \mathbb{R}^2 \setminus \Gamma,$$

$$\mathcal{D}\phi(x) := \int_\Gamma \psi(y) \frac{\partial}{\partial \nu_y} \Phi(x, y) \, \mathrm{d}s_y, \qquad x \in \mathbb{R}^2 \setminus \Gamma,$$

are single- and double-layer potentials, respectively. Then making use of the known jump relations of the single- and double-layer potentials across the boundary Γ, interpreted in the

sense of the trace theorem, we obtain the following expression for the Cauchy data of the solution on the boundary Γ:

$$u = -Ku + S\frac{\partial u}{\partial \nu} \tag{10}$$

$$\frac{\partial u}{\partial \nu} = -Tu + K'\frac{\partial u}{\partial \nu} \tag{11}$$

where S, K, K', T denote four basic boundary integral operators defined by

$$S\psi(x) := 2\int_\Gamma \psi(y)\Phi(x, y)\,\mathrm{d}s_y \qquad K\psi(x) := 2\int_\Gamma \psi(y)\frac{\partial}{\partial \nu_y}\Phi(x, y)\,\mathrm{d}s_y$$

$$K'\psi(x) := 2\int_\Gamma \psi(y)\frac{\partial}{\partial \nu_x}\Phi(x, y)\,\mathrm{d}s_y \qquad T\psi(x) := 2\frac{\partial}{\partial \nu_x}\int_\Gamma \psi(y)\frac{\partial}{\partial \nu_y}\Phi(x, y)\,\mathrm{d}s_y,$$

and Φ is the fundamental solution to the Helmholtz equation defined by

$$\Phi(x, y) := \frac{\mathrm{i}}{4}H_0^{(1)}(k|x - y|) \tag{12}$$

with $H_0^{(1)}$ being a Hankel function of the first kind of order zero.

For $|s| \leqslant 1/2$, S, K, K' and T are bounded operators having the following mapping properties:

$$S : H^{-1/2+s}(\Gamma) \longrightarrow H^{1/2+s}(\Gamma) \qquad K : H^{1/2+s}(\Gamma) \longrightarrow H^{1/2+s}(\Gamma) \tag{13}$$

$$K' : H^{-1/2+s}(\Gamma) \longrightarrow H^{-1/2+s}(\Gamma) \qquad T : H^{1/2+s}(\Gamma) \longrightarrow H^{-1/2+s}(\Gamma). \tag{14}$$

The mapping properties of the single- and double layer potential $\mathcal{S}$, D as well as of the above boundary operators in the case of non-smooth boundary are studied by Costabel in [6]. Note that in this case the operators K and K' are continuous, but not compact.

Adding (10) and (11) we arrive at the following expression:

$$\left(\frac{\partial u}{\partial \nu} + \mathrm{i}k\lambda u\right) = -Tu + K'\frac{\partial u}{\partial \nu} - \mathrm{i}k\lambda Ku + \mathrm{i}k\lambda S\frac{\partial u}{\partial \nu}. \tag{15}$$

We now denote by $\tilde{f} \in H^{1/2}(\Gamma)$ and $\tilde{h} \in H^{-1/2}(\Gamma)$ bounded extensions to the whole of Γ of the boundary data f, h (see theorem A4 of [11]), and write

$$u|_\Gamma = \psi_I + \tilde{f}, \tag{16}$$

and

$$\left.\frac{\partial u}{\partial \nu} + \mathrm{i}k\lambda u\right|_\Gamma = \psi_D + \tilde{h}, \tag{17}$$

or

$$\left.\frac{\partial u}{\partial \nu}\right|_\Gamma = \psi_D - \mathrm{i}k\lambda\psi_I + \tilde{h} - \mathrm{i}k\lambda\tilde{f}\,. \tag{18}$$

Obviously $\psi_I \in \tilde{H}^{1/2}(\Gamma_I)$ and $\psi_D \in \tilde{H}^{-1/2}(\Gamma_D)$, since $\psi_I \equiv 0$ on Γ_D and $\psi_D \equiv 0$ on Γ_I. The pair of functions ψ_I, ψ_D will be referred to as the unknown Cauchy data of a solution.

By now restricting (10) to Γ_I and (15) to Γ_D and using (16)–(18), we obtain a system of integral equations for the unknown Cauchy data

$$A\begin{pmatrix}\psi_D \\ \psi_I\end{pmatrix} = \boldsymbol{g} \tag{19}$$

where the operator A is given by

$$A = \begin{pmatrix} S_{DD}, & -K_{DI} - \mathrm{i}k\lambda S_{DI} \\ K'_{ID} + \mathrm{i}k\lambda S_{ID}, & k^2\lambda^2 S_{II} - \mathrm{i}k\lambda(K'_{II} + K_{II}) - T_{II} \end{pmatrix}, \tag{20}$$

and the right-hand side is given by

$$g = \begin{pmatrix} (\tilde{f} + K\tilde{f} + \mathrm{i}k\lambda S\tilde{f} - S\tilde{h})|_{\Gamma_D} \\ (\tilde{h} + T\tilde{f} + \mathrm{i}k\lambda K\tilde{f} - K'\tilde{h} + \mathrm{i}k\lambda K'\tilde{f} - \mathrm{i}k\lambda S\tilde{h} - k^2\lambda^2 S\tilde{f})|_{\Gamma_I} \end{pmatrix}. \tag{21}$$

Here the operator S_{ID} is the operator applied to a function ψ with supp $\subseteq \overline{\Gamma}_D$ and evaluated on Γ_I, with analogous definitions for S_{DD}, S_{DI}, S_{II}, K_{DI}, K'_{ID}, K_{II}, K'_{II} and T_{II}. The mapping properties (13), (14) imply that

$$\begin{aligned}
&S_{DD} : \tilde{H}^{-1/2}(\Gamma_D) \longrightarrow H^{1/2}(\Gamma_D) && S_{II} : \tilde{H}^{-1/2}(\Gamma_I) \longrightarrow H^{1/2}(\Gamma_I) \\
&S_{ID} : \tilde{H}^{-1/2}(\Gamma_D) \longrightarrow H^{1/2}(\Gamma_I) && K_{II} : \tilde{H}^{1/2}(\Gamma_I) \longrightarrow H^{1/2}(\Gamma_I) \\
&K'_{ID} : \tilde{H}^{-1/2}(\Gamma_D) \longrightarrow H^{-1/2}(\Gamma_I) && K'_{II} : \tilde{H}^{-1/2}(\Gamma_I) \longrightarrow H^{-1/2}(\Gamma_I) \\
&S_{DI} : \tilde{H}^{-1/2}(\Gamma_I) \longrightarrow H^{1/2}(\Gamma_D) && T_{II} : \tilde{H}^{1/2}(\Gamma_I) \longrightarrow H^{-1/2}(\Gamma_I). \\
&K_{DI} : \tilde{H}^{1/2}(\Gamma_I) \longrightarrow H^{1/2}(\Gamma_D).
\end{aligned}$$

Therefore, we have that the operator A maps continuously

$$\tilde{H}^{-1/2}(\Gamma_D) \times \tilde{H}^{1/2}(\Gamma_I) \longrightarrow H^{1/2}(\Gamma_D) \times H^{-1/2}(\Gamma_I).$$

It is clear that the system of integral equation (19) is equivalent to our original interior mixed boundary value problem (see [11]). Once the unknown Cauchy data are determined from (16) and (18) then the representation formula (9) determines the weak solution.

In the next lemma we will prove that the operator A is Fredholm with index zero and kern $A = \{0\}$. The latter, together with theorem 2.1, implies the solvability of the integral equation (19) and therefore of the original interior mixed boundary value problem (4*a*)–(4*c*). Since the operator $A : \tilde{H}^{-1/2}(\Gamma_D) \times \tilde{H}^{1/2}(\Gamma_I) \longrightarrow H^{1/2}(\Gamma_D) \times H^{-1/2}(\Gamma_I)$ is bijective, the inverse operator is bounded and furthermore the operators S, K, K', T involved in the right-hand side of (19) are bounded as well. Hence we may write

$$\|\psi_I\|_{\tilde{H}^{1/2}_{(\Gamma_I)}} + \|\psi_D\|_{\tilde{H}^{-1/2}_{(\Gamma_D)}} \leqslant C_1(\|\tilde{f}\|_{H^{1/2}_{(\Gamma)}} + \|\tilde{h}\|_{H^{-1/2}_{(\Gamma)}}). \tag{22}$$

The representation formula (9) now yields the following estimate for the weak solution u to (4*a*)–(4*c*):

$$\|u\|_{H^1(D)} \leqslant C_2\left(\|u\|_{H^{1/2}(\Gamma)} + \left\|\frac{\partial u}{\partial \nu}\right\|_{H^{-1/2}(\Gamma)}\right). \tag{23}$$

Combining (23) with (16) and (18), and then making use of (22) and of the boundness of the extension operator for the boundary data f, h we obtain the estimate (8). This ends the proof of the theorem. □

Lemma 2.4. *Let $H = \tilde{H}^{-1/2}(\Gamma_D) \times \tilde{H}^{1/2}(\Gamma_I)$, and its dual $H^* = H^{1/2}(\Gamma_D) \times H^{-1/2}(\Gamma_I)$. Then the operator $A : H \longrightarrow H^*$ given by (20) is Fredholm with index zero. In addition A has trivial kernel.*

Proof. It is known from [6], that the operators S and $-T$ are positive and bounded below up to a compact perturbation. In other words, there exist compact operators

$$L_S : H^{-1/2}(\Gamma) \longrightarrow H^{1/2}(\Gamma), \qquad L_T : H^{1/2}(\Gamma) \longrightarrow H^{-1/2}(\Gamma)$$

such that

$$\mathrm{Re}\,\langle (S + L_S)\psi, \bar{\psi}\rangle \geqslant C\|\psi\|^2_{H^{-1/2}(\Gamma)} \qquad \text{for} \quad \psi \in H^{-1/2}(\Gamma) \tag{24}$$

$$\mathrm{Re}\,\langle -(T + L_T)\psi, \bar{\psi}\rangle \geqslant C\|\psi\|^2_{H^{1/2}(\Gamma)} \qquad \text{for} \quad \psi \in H^{1/2}(\Gamma) \tag{25}$$

where the brackets $\langle \cdot, \cdot \rangle$ denote the duality between $H^{-1/2}(\Gamma)$ and $H^{1/2}(\Gamma)$.

Let us define $S_0 = S + L_S$ and $T_0 = -(T + L_T)$. Then S_0 and T_0 are bounded below and are positive. Then if $\psi = (\psi_D, \psi_I) \in H$ and $\tilde{\psi}_D \in H^{-1/2}(\Gamma)$, $\tilde{\psi}_I \in H^{1/2}(\Gamma)$ are the extension by zero on Γ of ψ_D and ψ_I, respectively, we define

$$A_0\psi = \begin{pmatrix} [(S_0\tilde{\psi}_D) - \mathrm{i}k\lambda(S_0\tilde{\psi}_I)]|_{\Gamma_D} - K_{DI}\psi_I \\ [\mathrm{i}k\lambda(S_0\tilde{\psi}_D) + k^2\lambda^2(S_0\tilde{\psi}_I) + (T_0\tilde{\psi}_I)]|_{\Gamma_I} + K'_{ID}\psi_D - \mathrm{i}k\lambda(K'_{II}\psi_I + K_{II}\psi_I) \end{pmatrix}$$

and

$$L_A\psi = \begin{pmatrix} (-L_S\tilde{\psi}_D + \mathrm{i}k\lambda L_S\tilde{\psi}_I)|_{\Gamma_D} \\ (L_T\tilde{\psi}_I - \mathrm{i}k\lambda L_S\tilde{\psi}_D - k^2\lambda^2 L_S\tilde{\psi}_I)|_{\Gamma_I} \end{pmatrix} \tag{26}$$

such that $A = (A_0 + L_A)$. In this way the operator $L_A : H \longrightarrow H^*$ is compact and $A_0 : H \longrightarrow H^*$ define the sesquilinear form

$$\begin{aligned} \langle A_0\psi, \bar{\psi}\rangle_{H,H^*} &= (S_0\tilde{\psi}_D, \tilde{\psi}_D)_\Gamma + k^2\lambda^2(S_0\tilde{\psi}_I, \tilde{\psi}_I)_\Gamma \\ &\quad -\mathrm{i}k\lambda(S_0\tilde{\psi}_I, \tilde{\psi}_D)_\Gamma + \mathrm{i}k\lambda(S_0\tilde{\psi}_D, \tilde{\psi}_I)_\Gamma \\ &\quad -(K_{DI}\psi_I, \psi_D)_{\Gamma_D} + (K'_{ID}\psi_D, \psi_I)_{\Gamma_I} \\ &\quad -\mathrm{i}k\lambda((K_{II} + K'_{II})\psi_I, \psi_I)_{\Gamma_I} + (T_0\tilde{\psi}_I, \tilde{\psi}_I)_\Gamma. \end{aligned} \tag{27}$$

Note that $(u, v)_{\Gamma_0}$, for $\Gamma_0 \subseteq \Gamma$ is the scalar product on $L^2(\Gamma_0)$ defined by $\int_{\Gamma_0} u\bar{v}\,\mathrm{d}s$. Let us now take the real part of (27). From (24) and the fact that supp $\tilde{\psi}_D \subseteq \Gamma_D$ and supp $\tilde{\psi}_I \subseteq \Gamma_I$, we obtain

$$\begin{aligned} &\mathrm{Re}\,[(S_0\tilde{\psi}_D, \tilde{\psi}_D)_\Gamma + k^2\lambda^2(S_0\tilde{\psi}_I, \tilde{\psi}_I)_\Gamma - \mathrm{i}k\lambda(S_0\tilde{\psi}_I, \tilde{\psi}_D)_\Gamma + \mathrm{i}k\lambda(S_0\tilde{\psi}_D, \tilde{\psi}_I)_\Gamma] \\ &\qquad = \mathrm{Re}\,(S_0(\tilde{\psi}_D - \mathrm{i}k\lambda\tilde{\psi}_I), (\tilde{\psi}_D - \mathrm{i}k\lambda\tilde{\psi}_I))_\Gamma \geqslant C\|\tilde{\psi}_D - \mathrm{i}k\lambda\tilde{\psi}_I\|^2_{H^{-1/2}(\Gamma)} \\ &\qquad = C(\|\psi_D\|^2_{\tilde{H}^{-1/2}(\Gamma_D)} + k^2\lambda^2\|\psi_I\|^2_{\tilde{H}^{1/2}(\Gamma_I)}). \end{aligned} \tag{28}$$

Furthermore, since K and K' are adjoint we have

$$\begin{aligned} \mathrm{Re}\,[-(K_{DI}\psi_I, \psi_D)_{\Gamma_D} + (K'_{ID}\psi_D, \psi_I)_{\Gamma_I}] &= \mathrm{Re}\,[-(K_{DI}\psi_I, \psi_D)_{\Gamma_D} + (\psi_D, K_{DI}\psi_I)_{\Gamma_D}] \\ &= \mathrm{Re}\,[-(K_{DI}\psi_I, \psi_D)_{\Gamma_D} + \overline{(K_{DI}\psi_I, \psi_D)}_{\Gamma_D}] = 0 \end{aligned} \tag{29}$$

and

$$\mathrm{Re}\,[-\mathrm{i}k\lambda((K_{II} + K'_{II})\psi_I, \psi_I)_{\Gamma_I}] = k\lambda\mathrm{Im}\,[(K_{II}\psi_I, \psi_I)_{\Gamma_I} + \overline{(K_{II}\psi_I, \psi_I)}_{\Gamma_I}] = 0.$$

Finally from (25) we have

$$\mathrm{Re}\,(T_0\tilde{\psi}_I, \tilde{\psi}_I)_\Gamma \geqslant C\|\tilde{\psi}_I\|^2_{H^{1/2}(\Gamma)} = C\|\psi_I\|^2_{H^{1/2}(\Gamma_I)}. \tag{30}$$

Combining (28)–(30) we conclude that

$$\mathrm{Re}\,\langle(A + L_A)\psi, \bar{\psi}\rangle_{H,H^*} \geqslant C\|\psi\|^2_H \qquad \text{for} \quad \psi \in \tilde{H}^{-1/2}(\Gamma_D) \times \tilde{H}^{1/2}(\Gamma_I) \tag{31}$$

where the operator L_A given by (26) is compact. We can now conclude that the operator A is Fredholm with index zero [11].

Next we show that kern $A = \{0\}$. To this end let $\psi = (\psi_D, \psi_I) \in \tilde{H}^{-1/2}(\Gamma_D) \times \tilde{H}^{1/2}(\Gamma_I)$ be a solution of the homogeneous equation $A\psi = 0$, and $\tilde{\psi}_D \in H^{-1/2}(\Gamma)$, $\tilde{\psi}_I \in H^{1/2}(\Gamma)$ their respective extensions by zero. Define the potential

$$v = \mathcal{S}\tilde{\psi}_D - \mathrm{i}k\lambda\mathcal{S}\tilde{\psi}_I - \mathcal{D}\tilde{\psi}_I, \tag{32}$$

which is a weak solution of the Helmholtz equation, i.e. $v \in \mathcal{L}_{\mathrm{int}}$, and $v \in \mathcal{L}_{\mathrm{ext}}$. Therefore by taking the normal derivative in (32) and approaching the boundary Γ from inside we obtain

$$2v|_\Gamma = \tilde{\psi}_I + S\tilde{\psi}_D - K\tilde{\psi}_I - \mathrm{i}k\lambda S\tilde{\psi}_I \tag{33}$$

$$2\left(\frac{\partial v}{\partial \nu} + \mathrm{i}k\lambda v\right)\Big|_\Gamma = \tilde{\psi}_D + K'\tilde{\psi}_D + \mathrm{i}k\lambda S\tilde{\psi}_D + k^2\lambda^2 S\tilde{\psi}_I - \mathrm{i}k\lambda(K + K')\tilde{\psi}_I - T\tilde{\psi}_I. \tag{34}$$

The integral equation $A\phi \equiv 0$ implies that

$$S\tilde{\psi}_D - K\tilde{\psi}_I - \mathrm{i}k\lambda S\tilde{\psi}_I|_{\Gamma_D} = 0,$$

and

$$K'\tilde{\psi}_D + \mathrm{i}k\lambda S\tilde{\psi}_D + k^2\lambda^2 S\tilde{\psi}_I - \mathrm{i}k\lambda(K + K')\tilde{\psi}_I - T\tilde{\psi}_I|_{\Gamma_I} = 0,$$

and since $\tilde{\psi}_I \equiv 0$ on Γ_D and $\tilde{\psi}_D \equiv 0$ on Γ_I, we have

$$v|_{\Gamma_D} \equiv 0, \qquad \left.\frac{\partial v}{\partial \nu} + \mathrm{i}k\lambda v\right|_{\Gamma_I} \equiv 0. \tag{35}$$

The latter means that (32) is a weak solution of the homogeneous interior mixed boundary problem, and hence, from theorem 2.1, $v \equiv 0$ in D.

Approaching the boundary from the outside one can show that (32) is also a weak solution of the homogeneous exterior mixed boundary problem. Hence, from theorem 2.2, $v \equiv 0$ in $\mathbb{R}^2 \setminus D$. Thus

$$\tilde{\psi}_I = v^+ - v^- = 0 \qquad \text{on} \quad \Gamma \tag{36}$$

$$\tilde{\psi}_D - \mathrm{i}k\lambda\tilde{\psi}_I = \frac{\partial v^+}{\partial \nu} - \frac{\partial v^-}{\partial \nu} = 0 \qquad \text{on} \quad \Gamma, \tag{37}$$

where the $\pm$ signs correspond to the interior and the exterior domain, respectively. Both (36), (37) imply that $\psi = (\psi_D, \psi_I) \equiv 0$ as a function in H. □

The following theorem will play a central role in the justification of the linear sampling method for solving the inverse scattering problem discussed in the following section.

Theorem 2.5. *The exterior mixed boundary value problem (3a)–(3d) has a weak solution in* $\mathcal{L}_{\text{ext}}$. *Moreover, the solution satisfies the estimate*

$$\|\chi u\|_{H^1(\mathbb{R}^2\setminus\overline{D})} \leqslant C(\|f\|_{H^{1/2}(\Gamma_D)} + \|g\|_{H^{-1/2}(\Gamma_I)}) \tag{38}$$

with C a positive constant and $\chi \in C^\infty_{\text{comp}}(\mathbb{R}^2 \setminus \overline{D})$ *an arbitrary cut-off function with compact support.*

Proof. The proof of the theorem proceeds in exactly the same way as for theorem 2.3 with the only modifications coming from reversing the signs of the operators K and K', respectively, in (10) and (11). □

3. Inverse scattering problem

We now consider the scattering of an electromagnetic time harmonic wave by a perfectly conducting infinite cylinder that is partially coated by a material with surface impedance λ. Assuming the electric field is polarized in the TM mode and the plane wave is propagating in the direction d, the scattered field u (after factoring out a term of the form $\mathrm{e}^{-\mathrm{i}\omega t}$ where ω is the frequency) satisfies the exterior mixed boundary value problem (3*a*)–(3*d*) with $f := -\mathrm{e}^{\mathrm{i}kx\cdot d}$ and $h := -\left(\frac{\partial}{\partial \nu} + \mathrm{i}k\lambda\right)\mathrm{e}^{\mathrm{i}kx\cdot d}$. It is easy to show [1] that the scattered field has the asymptotic behaviour

$$u(x) = \frac{\mathrm{e}^{\mathrm{i}kr}}{\sqrt{r}} u_\infty(\hat{x}, d) + \mathrm{O}(r^{-3/2}) \tag{39}$$

where u_∞ is the *far-field pattern* of the scattered wave.

The inverse scattering problem we will consider in this section of our paper is to determine D from a knowledge of $u_\infty(\hat{x}, d)$ for $\hat{x}$ and d on the unit circle Ω.

Before proceeding to the inverse problem, we need to generalize the approximation result of [5] to the case of Lipschitz boundary.

As in [5] for $n = 0, \pm 1, \pm 2, \ldots$ we define u_n by

$$u_n(x) := J_n(kr)\, \mathrm{e}^{\mathrm{i}n\theta} \tag{40}$$

where J_n is a Bessel function of order n and (r, θ) are the polar coordinates of $x \in \mathbb{R}^2$.

A *Herglotz wavefunction* is a solution of the Helmholtz equation of the form

$$v_g(x) := \int_\Omega \mathrm{e}^{\mathrm{i}kx\cdot d} g(d)\, \mathrm{d}s(d), \tag{41}$$

where Ω is the unit sphere and $g \in L^2(\Omega)$ is the Herglotz kernel of v_g.

Then, if $\{a_n\} \in l^2$

$$v(x) := \sum_{-\infty}^{\infty} a_n u_n(x) \tag{42}$$

is a Herglotz wavefunction.

Theorem 3.1. *Let $D \subset \mathbb{R}^2$ be a bounded domain with Lipschitz boundary Γ containing the origin, such that $\mathbb{R}^2 \setminus \overline{D}$ is connected. Then with respect to the $H^1(D)$ norm the set of Herglotz wavefunctions is dense in the space of the variational solutions $\mathcal{L}_{\mathrm{int}}$ of the Helmholtz equation.*

Proof. First we observe that the set $\{\frac{\partial u_n}{\partial \nu} + \mathrm{i}u_n\}$ is complete in $H^{-1/2}(\Gamma)$. This can be shown exactly in the same way as in the theorem 1 in [5] for the case of a smooth boundary since the proof is based only on the facts that the single-layer potential $\mathcal{S} : H^{-1/2}(\Gamma) \longrightarrow H^1_{\mathrm{loc}}(\mathbb{R}^2)$ and double-layer potential $\mathcal{D} : H^{1/2}(\Gamma) \longrightarrow H^1_{\mathrm{loc}}(\mathbb{R}^2 \setminus \overline{D})$ and $\mathcal{D} : H^{1/2}(\Gamma) \longrightarrow H^1(D)$ are continuous and satisfy the well known jump relations interpreted in terms of the trace theorem.

Now let $u \in \mathcal{L}_{\mathrm{int}}$ be a weak solution of the Helmholtz equation. Then by the trace theorem $\phi = \frac{\partial u}{\partial \nu} + \mathrm{i}u \in H^{-1/2}(\Gamma)$, and so ϕ can be approximated in $H^{-1/2}(\Gamma)$ by $\tau = \frac{\partial v}{\partial \nu} + \mathrm{i}v$ where v is a Herglotz wavefunction. An application of theorem 2.3 to the particular case when $\lambda = 1/k$ and $\Gamma_D = \emptyset$ yields

$$\|u - v\|_{H^1(D)} \leqslant C \|\phi - \tau\|_{H^{-1/2}(\Gamma)}$$

where C is a positive constant which proves the theorem. □

Theorem 3.1 will play a central role in the linear sampling method [3, 4, 9] for solving the inverse scattering problem for partially coated obstacles, i.e. the scattered field u satisfies the exterior mixed boundary value problem (3*a*)–(3*d*) with $f := -\mathrm{e}^{\mathrm{i}kx\cdot d}$ and $h := -\left(\frac{\partial}{\partial \nu} + \mathrm{i}k\lambda\right) \mathrm{e}^{\mathrm{i}kx\cdot d}$. In particular, for $z \in D$, the linear sampling method looks for a solution $g = g(\cdot, z) \in L^2(\Omega)$ of the far-field equation

$$\int_\Omega u_\infty(\hat{x}, d) g(d, z)\, \mathrm{d}s(d) = \gamma \mathrm{e}^{-\mathrm{i}k\hat{x}\cdot z} \tag{43}$$

where

$$\gamma = \frac{\mathrm{e}^{\mathrm{i}\pi/4}}{\sqrt{8\pi k}}. \tag{44}$$

Then, noting that $\gamma \mathrm{e}^{-\mathrm{i}k\hat{x}\cdot z}$ is the far-field pattern of the fundamental solution $\Phi(x, z)$, we see by Rellich's lemma that if a solution to (43) exists then

$$\int_\Omega u(x, d) g(d, z)\, \mathrm{d}s(d) = \Phi(x, z) \tag{45}$$

for $x \in \mathbb{R}^2 \setminus D$ and in particular for $x \in \Gamma$. Since $u(x, d)$ is in $L^\infty(\Gamma)$, if we now let $z \to \Gamma$ then from (45) we see that $\|g(\cdot, z)\|_{L^2(\Omega)}$ becomes unbounded as $z \to \Gamma$ since $\Phi(x, z)$ becomes

unbounded as $z \to \Gamma$. Thus Γ is characterized by the fact that the solution of (43), if it exists, becomes unbounded as $z \to \Gamma$.

Unfortunately, in general a solution to (43) does not exist! However, from theorem 3.1 the solution of interior mixed boundary value problem (4*a*)–(4*c*) with $f := -\Phi(\cdot, z)$ and $h := -\left(\frac{\partial}{\partial \nu} + \mathrm{i}k\lambda\right)\Phi(\cdot, z)$, $z \in D$, can be approximated in $H^1(D)$ by a Herglotz wavefunction v_g. Since the trace operator is bounded from $H^1(D)$ to $H^{1/2}(\Gamma)$, then f and h are approximated in $H^{1/2}(\Gamma)$ and $H^{-1/2}(\Gamma)$ by $v_g|_{\Gamma_D}$ and $\left(\frac{\partial}{\partial \nu} + \mathrm{i}k\lambda\right) v_g|_{\Gamma_I}$, respectively. It now follows from theorem 2.5 and the Green formula that the Herglotz kernel g of v_g is an approximate solution of (43), i.e. if we write (43) in the form

$$Fg = \Phi_\infty(\cdot, z), \tag{46}$$

then for every $\epsilon > 0$ there exists a $g \in L^2(\Omega)$, $g = g(\cdot, z)$, such that

$$\|Fg - \Phi_\infty(\cdot, z)\|_{L^2(\Omega)} < \epsilon. \tag{47}$$

Furthermore, for this g it follows from the boundness of the trace operator and the fact that, for $z \in \Gamma$, $\Phi(\cdot, z)$ is not in $H^1(D)$ that

$$\lim_{z \to \Gamma} \|v_g\|_{H^1(D)} = \infty \tag{48}$$

and hence

$$\lim_{z \to \Gamma} \|g(\cdot, z)\|_{L^2(\Omega)} = \infty. \tag{49}$$

The linear sampling method is to now use the Morozov discrepancy principle to solve (46) and determine Γ from the condition (49). Details of how this is done numerically will be provided in the next section of this paper.

A drawback of the above analysis is that we require that $z \in D$, i.e. nothing is said about what happens when $z \in \mathbb{R}^2 \setminus \overline{D}$. Indeed it was this concern that led Kirsch to develop a second version of the linear sampling method that is only valid for the case of a non-absorbing boundary condition, but on the other hand allows z to be either in D or $z \in \mathbb{R}^2 \setminus \overline{D}$ [9]. However, in our numerical examples it is seen that for $z \in \mathbb{R}^2 \setminus \overline{D}$ the regularized solution g of the far-field equation is in fact much larger than it is for $z \in D$. We now give an explanation of this behaviour for the special case when $\Gamma_I = \emptyset$ and Γ is in class C^2, i.e. the same case considered by Kirsch in [9] for his modified linear sampling method. In particular, assume that $\Gamma_I = \emptyset$, $\Gamma \in C^2$, and k^2 is not a Dirichlet or Neumann eigenvalue for D. Then if $z \in \mathbb{R}^2 \setminus \overline{D}$ we see that $\Phi_\infty(\hat{x}, z) = \gamma \mathrm{e}^{-\mathrm{i}k\hat{x}\cdot z}$ is not the far-field pattern of a radiating solution of the Helmholtz equation defined in the exterior of D.

On the other hand, let us define the far-field operator $\mathcal{F} : L^2(\Gamma) \longrightarrow L^2(\Omega)$

$$(\mathcal{F}\varphi)(\hat{x}) := \int_\Gamma \varphi(y) \frac{\partial}{\partial \nu_y} \mathrm{e}^{-\mathrm{i}k\hat{x}\cdot y}\, \mathrm{d}s(y). \tag{50}$$

Obviously the adjoint operator $\mathcal{F}^* : L^2(\Omega) \longrightarrow L^2(\Gamma)$ is given by

$$(\mathcal{F}^*\psi)(y) := \frac{\partial}{\partial \nu_y} \int_\Omega \psi(\hat{x}) \mathrm{e}^{\mathrm{i}k\hat{x}\cdot y}\, \mathrm{d}s(\hat{x}). \tag{51}$$

By proceeding as in theorem 5.17 of [1] (the normal derivative of the single-layer potential has to be replaced by the double-layer potential and the rest works exactly in the same way) it can be proved that the far-field operator (50) is injective with dense range. Hence using Tikhonov regularization we can construct a regularized solution of

$$(\mathcal{F}\varphi)(\hat{x}) := \mathrm{e}^{-\mathrm{i}k\hat{x}\cdot z} \tag{52}$$

such that (52) is approximately satisfied for small values of the regularization parameter. In particular, if $\varphi_\alpha \in L^2(\Gamma)$ is the regularized solution of (52) corresponding to the regularization

parameter α (chosen by a regular regularization strategy, e.g. the Morozov discrepancy principle),

$$\lim_{\alpha\to 0} \|\varphi_\alpha\|_{L^2(\Gamma)} = \infty. \tag{53}$$

Then from theorem 5.5 of [1] and the Jacobi–Anger expansion [1, p 67] there exists a Herglotz wavefunction v_g with kernel g such that v_g approximates $-1/2\,(\varphi_\alpha + K\varphi_\alpha)$ in $L^2(\Gamma)$. By theorem 3.21 of [1] and the fact that (50) is the far-field pattern of $\gamma^{-1}\mathcal{D}\varphi$ we see that $(Fg)(\hat{x}) \approx \gamma \mathrm{e}^{-\mathrm{i}k\hat{x}\cdot z}$ for small values of α. Since k^2 is not a Neumann eigenvalue, $I + K$ has a bounded inverse in $L^2(\Gamma)$ (see the proof of theorem 3.20 of [1]), and from (53) we can conclude that

$$\lim_{\alpha\to 0} \|v_g\|_{L^2(\Gamma)} = \infty. \tag{54}$$

This implies that

$$\lim_{\alpha\to 0} \|g(\cdot, z)\|_{L^2(\Omega)} = \infty \tag{55}$$

for any $z \in \mathbb{R}^2\backslash\overline{D}$, thus providing an explanation for the numerical examples in the next section of this paper for the case when $z \in \mathbb{R}^2\backslash\overline{D}$, Γ is smooth with $\Gamma_I = \emptyset$, and k^2 is not a Dirichlet or Neumann eigenvalue.

The above results can be also obtained for the cases of Neumann and impedance boundary value problems by using the far-field operator $\mathcal{F} : L^2(\Gamma) \longrightarrow L^2(\Omega)$ defined by

$$(\mathcal{F}\varphi)(\hat{x}) := \int_\Gamma \varphi(y)\mathrm{e}^{-\mathrm{i}k\hat{x}\cdot y}\mathrm{d}s(y) \tag{56}$$

instead of (50).

4. Numerical examples

Here we shall show some results of numerical experiments to reconstruct partially coated objects. The far-field data are synthetic, but corrupted by random noise. Rather than using the integral equation approach to the forward problem outlined earlier, we modified an existing code for the scattering problem that uses cubic isoparametric finite elements. We shall describe this approach next.

The method we have in mind is an extension of the finite element–spectral method described in [10]. First we introduce an auxiliary domain, the disc B_R of radius R containing $\overline{D}$ in its interior. We shall need to refer to the boundary of B_R which we denote Σ_R. The computational domain is the bounded domain $\Omega_R = B_R\backslash\overline{D}$. The solution u of (5) can then be decomposed into two components

$$u_1 = u|_{\Omega_R} \qquad \text{and} \qquad u_2 = u|_{\mathbb{R}^2\backslash\overline{\Omega_R}}.$$

The component $u_1 \in H^1(\Omega_R)$ satisfies $u_1|_{\Gamma_D} = f$ and

$$\int_{\Omega_R} \nabla u_1 \cdot \nabla\bar{v}\,\mathrm{d}x - k^2 \int_{\Omega_R} u_1\bar{v}\,\mathrm{d}x - \mathrm{i}k\lambda(u_1, v)_{\Gamma_I} - \mathrm{i}k(u_1, v)_{\Sigma_R} = -\langle h, \bar{v}|_{\Gamma_I}\rangle + \langle\gamma, \bar{v}|_{\Sigma_R}\rangle, \tag{57}$$

where $\gamma \in H^{-1/2}(\Sigma_R)$ is a function that must be determined. It turns out in fact that

$$\gamma = \frac{\partial u}{\partial r} - \mathrm{i}ku \qquad \text{on} \quad \Sigma_R.$$

In the exterior domain, $u_2 \in H^1_{\text{loc}}(\mathbb{R}^2 \setminus \overline{B_R})$ is the weak solution of

$$\Delta u_2 + k^2 u_2 = 0 \qquad \text{in} \quad \mathbb{R}^2 \setminus \overline{B_R}, \tag{58a}$$

$$\frac{\partial u_2}{\partial r} - \mathrm{i}k u_2 = \gamma \qquad \text{on} \quad \Sigma_R, \tag{58b}$$

$$\frac{\partial u_2}{\partial r} - \mathrm{i}k u_2 = \mathrm{o}\left(\frac{1}{\sqrt{r}}\right) \qquad \text{as} \quad r \to \infty. \tag{58c}$$

Since we want u to be continuous across Σ_R, γ must be chosen so that

$$u_1 = u_2 \qquad \text{on} \quad \Sigma_R.$$

The numerical method is derived from these equations as follows. We assume that the domain D is a smooth curvilinear polygon. First the domain Ω_R is approximately covered by a mesh of cubic isoparametric triangles. We assume that there are finitely many points in Π (see the beginning of section 2) and that these points are vertices of the triangulation. The function $u_{1,h}$ is then taken to be a cubic isoparametric finite-element function that interpolates f on Γ_D using interpolation at mapped Gauss–Lobatto quadrature points (see [13]). This function satisfies the discrete weak equations

$$\int_{\Omega_R} \nabla u_{1,h} \cdot \nabla \bar{v}_h \, \mathrm{d}x - k^2 \int_{\Omega_R} u_{1,h} \bar{v}_h \, \mathrm{d}x - \mathrm{i}k\lambda \left(u_{1,h}, v_h\right)_{\Gamma_I} - \mathrm{i}k \left(u_{1,h}, v_h\right)_{\Sigma_R}$$
$$= -\langle h, \bar{v}_h|_{\Gamma_I} \rangle + \langle \gamma_N, \bar{v}_h|_{\Sigma_R} \rangle, \tag{59}$$

for all cubic isoparametric elements v_h that interpolate zero on Γ_D. The unknown function γ_N is taken to be a finite trigonometric sum,

$$\gamma_N = \sum_{n=-N}^{N} g_n \exp(\mathrm{i}n\theta). \tag{60}$$

Because of this special choice, we can then compute a discrete exterior field $u_{2,N}$ by solving (58) with γ_N in place of γ. This can be done using a Hankel function expansion, so $u_{2,N}$ is computed exactly. The unknown function γ_N is then found by requiring that

$$P_N u_{1,h} = u_{2,N} \qquad \text{on} \quad \Sigma_R$$

where P_N is the $L^2(\Sigma_R)$ orthogonal projection onto the space of finite trigonometric series used in (60). The implementation we use computes the capacitance matrix for this problem by solving $2N + 1$ interior finite-element problems (one for each basis function of γ_N). Once the matrix for (60) has been set up and factored, γ_N can be found for different f and g at the expense of one further finite-element solve per pair of data. The far-field pattern can be easily found from γ_N using $u_{2,N}$.

Because of the singularity in the solution generated by transitions between Dirichlet and impedance data on Π, the analysis of [10] is not directly applicable. The singularity also implies the need to refine the mesh close to Π. We have done this manually, but have not attempted an adaptive approach to this problem. The extension of the error analysis and analysis of optimal grids for this problem is an interesting project motivated by this paper.

For the inverse problem we select a domain D, boundaries Γ_D and Γ_I and impedance λ. Then, using the incident field $\exp(\mathrm{i}k\boldsymbol{x} \cdot \boldsymbol{d})$ where $|\boldsymbol{d}| = 1$ we can compute the data h and g and by solving the finite-element problem compute the far-field pattern. This is obtained as a trigonometric series

$$u_\infty = \sum_{n=-N}^{N} u_{\infty,n} \exp(\mathrm{i}n\theta).$$

Of course, these coefficients are already in error by the discretization error of the finite-element–spectral method. However, we also add random noise to the Fourier coefficients by

$$u_{\infty,a,n} = u_{\infty,n}(1 + \epsilon\chi_n)$$

where ϵ is a parameter (in the results we report here $\epsilon = 0.05$) and χ_n is given by a random number generator that provides uniformly distributed random numbers in the interval $[-1, 1]$. This avoids inverse crimes. Thus the input to the inverse solver is the approximate far-field pattern

$$u_{\infty,a} = \sum_{n=-N}^{N} u_{\infty,a,n} \exp(\mathrm{i}n\theta).$$

The inverse problem is then solved using Tikhonov regularization and the Morozov discrepancy principle as described in [3]. In particular, using the above expression for $u_{\infty,a}$, the far-field equation (43) is rewritten as an ill-conditioned matrix equation for the Fourier coefficients of g which we write in the form

$$A\vec{g}_z = \vec{f}_z\,. \tag{61}$$

As already noted, this equation needs to be regularized. We start by computing the singular value decomposition of A

$$A = U\Lambda V^*$$

where U and V are unitary and Λ is real diagonal with $\Lambda_{\ell,\ell} = \sigma_\ell$, $1 \leqslant \ell \leqslant n$. The solution of (61) is then equivalent to solving

$$\Lambda V^*\vec{g}_z = U^*\vec{f}_z\,. \tag{62}$$

Let

$$\vec{\rho}_z = (\rho_{z,1}, \rho_{z,2}, \ldots, \rho_{z,n})^{\mathrm{T}} = U^*\vec{f}_z.$$

Then the Tikhonov regularization of (62) leads to solving

$$\min_{\vec{g}_z \in \mathbb{R}^n} \|\Lambda V^*\vec{g}_z - \vec{f}_z\|_{\ell^2}^2 + \alpha\,\|\vec{g}\|_{\ell^2}^2$$

where $\alpha > 0$ is the Tikhonov regularization parameter. Defining $\vec{u}_z = V^*\vec{g}_z$, we see that the solution to the problem is

$$u_{z,\ell} = \frac{\sigma_\ell}{\sigma_\ell^2 + \alpha}\rho_{z,\ell}, \qquad 1 \leqslant \ell \leqslant n,$$

and hence

$$\|\vec{g}_z\|_{\ell^2} = \|\vec{u}_z\|_{\ell^2} = \left(\sum_{\ell=1}^{n} \frac{\sigma_\ell^2}{(\alpha + \sigma_\ell^2)^2}\,|\rho_{z,\ell}|^2\right)^{1/2}.$$

Note we use the discrete ℓ_2 norm of $\vec{g}_z$ rather than the $L^2(\Omega)$ norm of g. The regularization parameter α depends on both z and the error in the data $\{u_{\infty,a}\}$. As mentioned previously, we use the Morozov discrepancy principle to determine α. Suppose we know an estimate for the error in the far-field operator so that

$$\|F - F_h^a\| \leqslant \delta$$

for some $\delta > 0$ (using the operator norm induced by $L^2(\Omega)$). Then the Morozov procedure picks $\alpha = \alpha(z)$ to be the zero of

$$m_z(s) = \sum_{j=1}^{n} \frac{\delta^2\sigma_j^2 - s^2}{(s + \sigma_j^2)^2}\,|\rho_{z,j}|^2, \qquad s > 0.$$

For this report, we select one of two scatterers shown in figure 1 (the single bullet or the double bullet). Different choices of boundary condition are used:

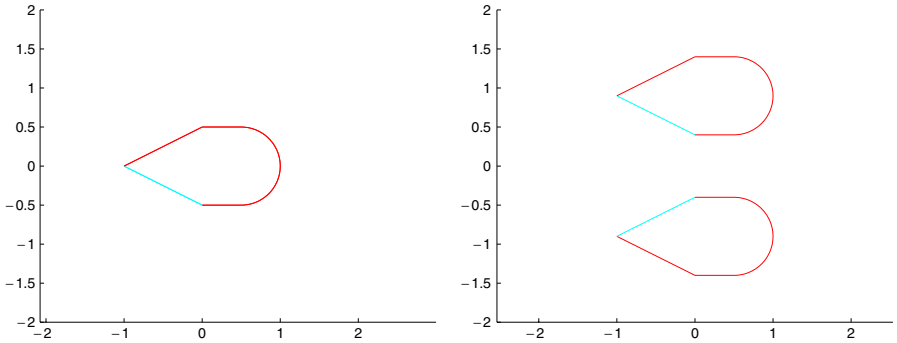

Figure 1. The boundary of the scatterers used in this study. When mixed boundary conditions are used the blue portion of the boundary is Γ_I and has an impendance boundary condition, while the red portion is Γ_D and has a Dirichlet boundary condition.

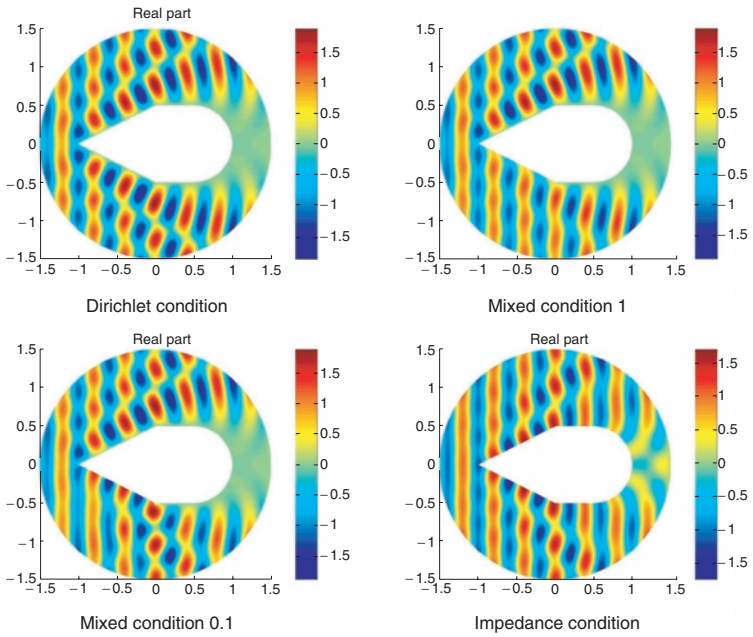

Figure 2. Here we show the real part of the total field when $k = 15.7$ for incident field $\exp(ikx)$. Red regions correspond to positive values of Re (u) and blue to negative values. For the definition of each problem, see the text. The strong singularity near the junction between Γ_D and Γ_I is clearly visible as a rapid variation in contours near these points.

Dirichlet condition. In this case $\Gamma_D = \Gamma$. This case is intended as a baseline for comparison since most of our previous work has concentrated on the Dirichlet problem.

Mixed condition 1. Here an impedance boundary condition with $\lambda = 1$ is used on the cyan portion of the appropriate boundary in figure 1.

Mixed condition 0.1. Here an impedance boundary condition with $\lambda = 0.1$ is used on the cyan portion of the appropriate boundary in figure 1.

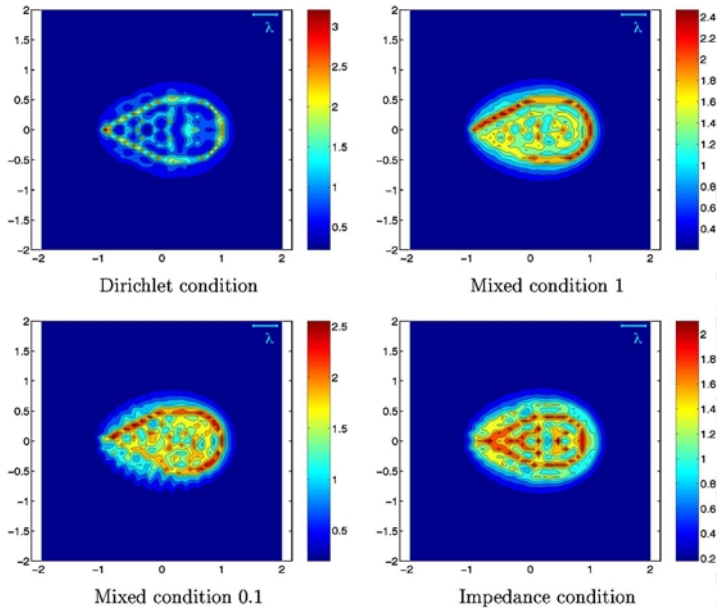

Figure 3. Here we show the reconstruction of the single bullet when $k = 15.7$ by plotting contours of $1/||g||_{L^2(\Omega)}$. The line segment marked λ in the upper right-hand corner of the figure is the wavelength.

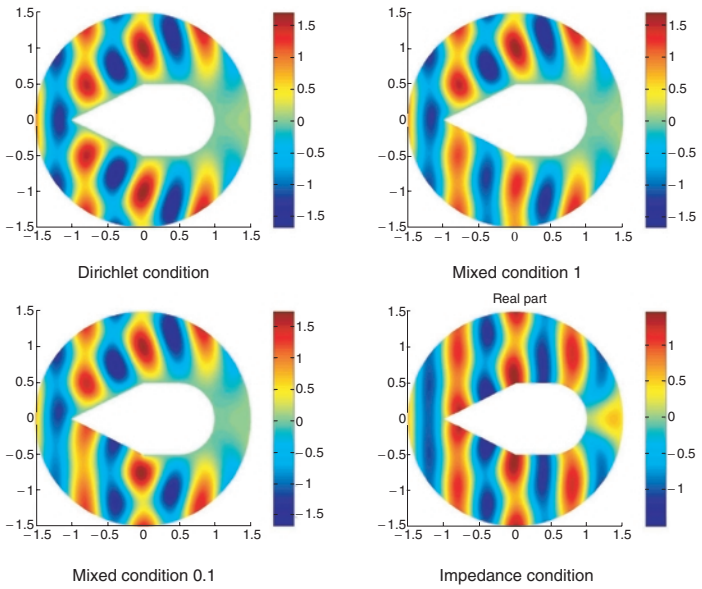

Figure 4. Here we show the real part of the total field when $k = 7.85$ for incident field $\exp(ikx)$. Again the singularity is visible at the junction between Dirichlet and impedance data.

Impedance condition. Here an impedance boundary condition with $\lambda = 0.1$ is used on the entire boundary.

Our first results, in figure 2, show the real part of the total field for the forward problem

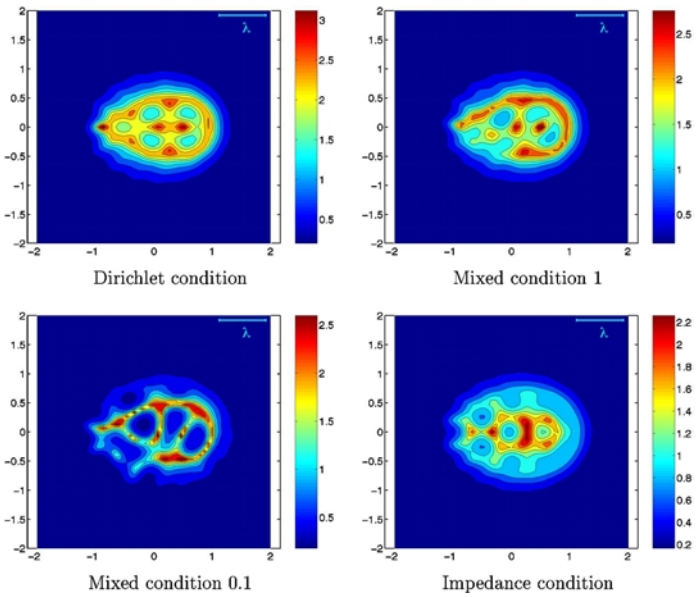

Figure 5. Here we show the reconstruction of a single bullet when $k = 7.85$ by plotting contours of $1/||g||_{L^2(\Omega)}$. The line segment marked λ in the upper right-hand corner of the figure is the wavelength.

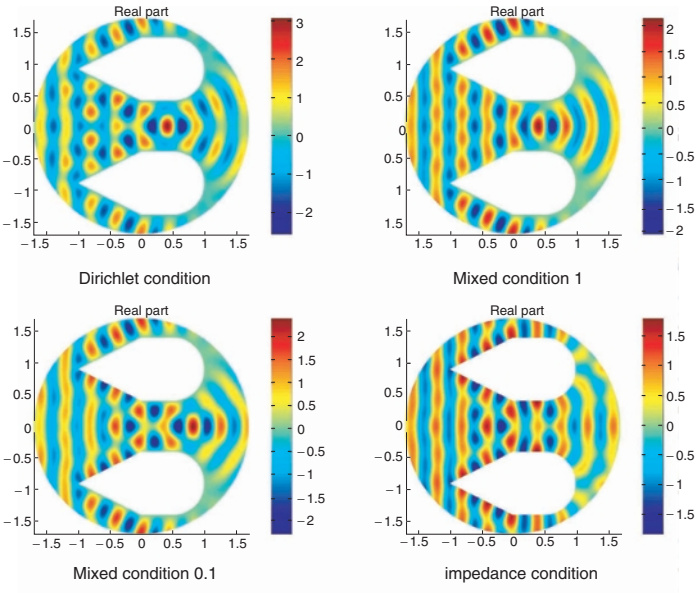

Figure 6. Here we show the real part of the total field when $k = 15.7$ for incident field $\exp(\mathrm{i}kx)$ using the double bullet scatterer.

for a single bullet when $k = 15.7$ and the direction $\boldsymbol{d} = (1, 0)^{\mathrm{T}}$. For the mixed problems, the strong singularity near the junction between Γ_D and Γ_I is clearly visible as a rapid variation in contours near these points.

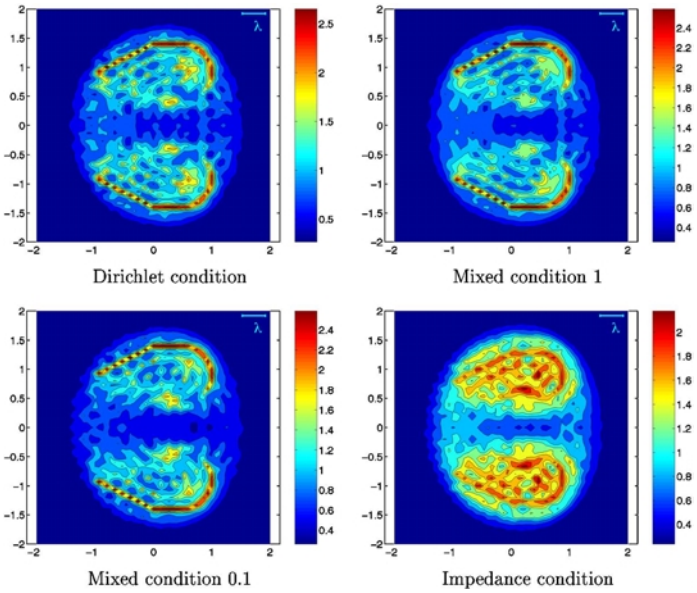

Figure 7. Here we show the reconstruction of the double bullet when $k = 15.7$ by plotting contours of $1/||g||_{L^2(\Omega)}$. The line segment marked λ in the upper right-hand corner of the figure is the wavelength.

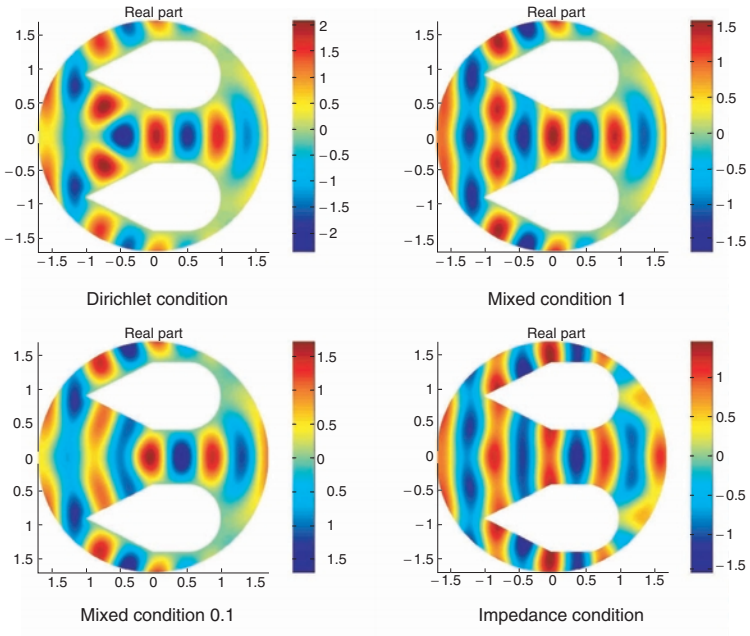

Figure 8. Here we show the real part of the total field when $k = 7.85$ for incident field $\exp(ikx)$ using the double bullet target.

Using data for $k = 15.7$ and 64 incoming waves (with the addition of noise) in the linear sampling method we obtain the reconstructions shown in figure 3. The addition of noise results

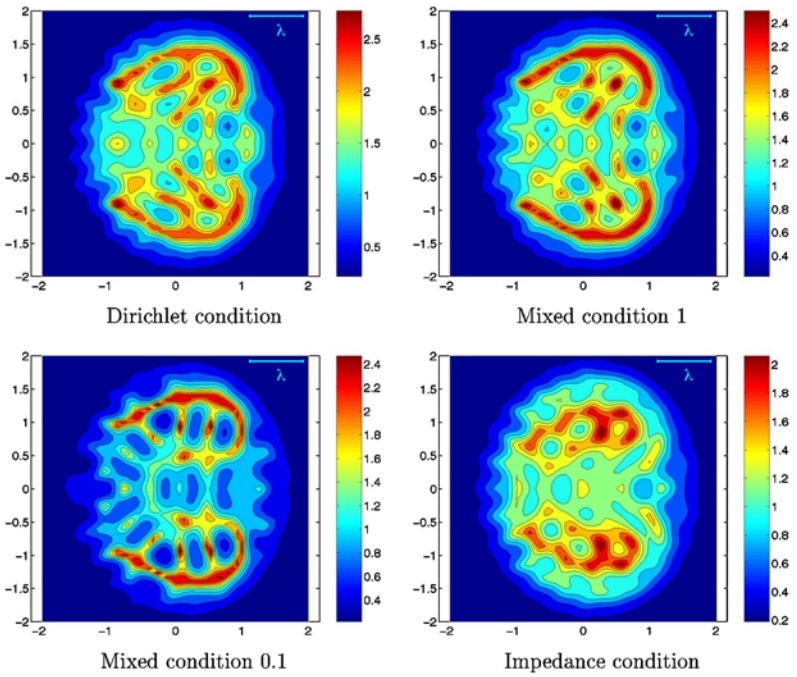

Figure 9. Here we show the reconstruction of the double bullet when $k = 7.85$ by plotting contours of $1/||g||_{L^2(\Omega)}$. The line marked λ in the upper right-hand corner of the figure is the wavelength.

in a relative spectral norm error of between 4 and 5% in the discrete matrix corresponding to F. To obtain the results in figure 3 we discretized g using a trigonometric series with 97 modes. The sampling domain is the square $[-2, 2]^2$ and we use a uniform grid for the sampling point z with 61 points in x and y. From the reconstructions it is apparent that Dirichlet boundary conditions give the best reconstruction. The mixed cases show a poorer reconstruction of the impedance face Γ_I, but in all cases the boundary of the single bullet is convincingly reconstructed.

Next we consider a lower wavenumber, $k = 7.85$. Since the wavelength is longer compared with the scatterer we would expect a decrease in the resolution of the reconstruction. The data error due to adding noise to the computed far-field pattern results in a relative spectral norm error of between 3.8 and 4.3%. Results for the forward problem are shown in figure 4 and for the inverse problem in figure 5.

Next we turn to examine the disconnected target denoted the double bullet in figure 1. A strength of the linear sampling method is that we do not need to know how many targets are present in order to correctly parametrize the boundary. We also do not need to know the boundary condition. Here we show some results for the double bullet with similar boundary data to that used for our study of the single bullet. We emphasize the fact that neither the number of components nor the boundary condition on each component need be known *a priori*. We start with $k = 15.7$ and show forward data for the various boundary conditions in figure 6. Using data (again 64 incoming waves) for this figure, with noise, we produce the reconstructions shown in figure 7. The data error for these reconstructions is between 4.6 and 4.9% in the relative spectral norm.

From figure 7 it is clear that we can distinguish two scatterers and can see the gap

between the two bullets. Unfortunately, in no case are the facing surfaces of the two scatterers reconstructed cleanly. Strangely, the impedance case gives the best indication of the extent of the two scatterers.

If we decrease the wavenumber sufficiently far, it is impossible to distinguish the two bullets (as is to be expected). When we use $k = 7.85$ the blurring of the two scatterers is starting to become apparent. For completeness we show data for the forward problem in figure 8. The results of the linear sampling method are shown in figure 9. Here the data error for the reconstructions is between 4.0 and 4.1%. Except for the case of a full impedance boundary condition, the outer surface is reconstructed well, but the channel between the scatterers has all but vanished.

Acknowledgments

The research of DC and PM was supported in part by a grant from the Air Force Office of Scientific Research. FC was supported in part by NSF grant 9631287 at the University of Delaware.

References

[1] Colton D and Kress R 1998 *Inverse Acoustic and Electromagnetic Scattering Theory* 2nd edn (Berlin: Springer)
[2] Colton D, Coyle J and Monk P 2000 Recent developments in inverse acoustic scattering theory *SIAM Rev.* **42** 369–414
[3] Colton D, Piana M and Potthast R 1997 A simple method using Morozov's discrepancy principle for solving inverse scattering problems *Inverse Problems* **13** 1477–93
[4] Colton D and Kirsch A 1996 A simple method for solving inverse scattering problems in the resonance region *Inverse Problems* **12** 383–93
[5] Colton D and Sleeman B D 2000 An approximation property of importance in inverse scattering theory *Proc. Edinburgh Math. Soc.* at press
[6] Costabel M 1988 Boundary integral operator on Lipschitz domains: elementary results *SIAM J. Math. Anal.* **19** 613–26
[7] Hsiao G and Wendland W 1977 A finite element method for some integral equations of the first kind *J. Math. Anal. Appl.* **58** 449–81
[8] Hsiao G and Wendland W 1979 On integral equation method for the plane mixed boundary value problem for the Laplacian *Math. Methods Appl. Sci.* **1** 265–321
[9] Kirsch A 1998 Characterization of the shape of a scattering obstacle using the spectral data of the far-field operator *Inverse Problems* **14** 1489–512
[10] Kirsch A and Monk P 1990 Convergence analysis of a coupled finite element and spectral method in acoustic scattering *IMA J. Numer. Anal.* **9** 425–47
[11] McLean W 2000 *Strongly Elliptic Systems and Boundary Integral Equations* (Cambridge: Cambridge University Press)
[12] Nédélec J C 1976 Curved finite element methods for the solution of singular integral equations on surface in $\mathbb{R}^3$ *Comput. Methods Appl. Mech. Eng.* **8** 61–80
[13] Scott R 1975 Interpolated boundary conditions in the finite element method *SIAM J. Numer. Anal.* **12** 404–27